J. Jpn. Soc. Powder Powder Metallurgy, **72** (2025) S353-S360
https://doi.org/10.2497/jjspm.15A-T7-04

Recycling of Ti-6Al-4V Powder in Metal Binder Jetting

Kevin JANZEN[1]*, Kim Julia KALLIES[2], Lennart WAALKES[1], Philipp IMGRUND[1] and Claus EMMELMANN[3]

[1]Fraunhofer Research Institution for Additive Manufacturing Technologies IAPT,
Am Schleusengraben 14, 21029 Hamburg, Germany.
[2]Frankfurt University of Applied Sciences, Nibelungenpl. 1, 60318 Frankfurt am Main, Germany.
[3]Institute of Laser and System Technologies (iLAS), Hamburg University of Technology TUHH, Harburger Schloßstr. 28, 21079 Hamburg, Germany.

Abstract
Powder in sinter-based metal binder jetting is not fused but only bonded, which in principle ensures full reusability of the unbonded powder. This increases both resource and cost efficiency. In order to explore this potential, this study investigates the effect of powder recycling with regard to handling and thermal influences. For this purpose, a gas atomized Ti-6Al-4V powder is used as a reference powder. It is shown that recycling the Ti-6Al-4V powder four times leads to a minor change in the particle size distribution and an improvement in flow properties. No differences in the average green part densities could be determined, but an increase in their range (from 1 % to up to 7 %). Furthermore, it is demonstrated that the thermal influence due to curing and conditioning (temperatures ≤ 200°C) after printing does not lead to a significant increase in oxygen or nitrogen even after 15 repetitions.

Keywords: metal binder jetting; powder recycling; titanium alloys.

Introduction

The introduction of metal binder jetting (MBJ) for industrial use has been anticipated as a significant disruptor, potentially lowering production costs dramatically compared to laser or electron beam powder bed fusion (L/E-PBF). This cost reduction is facilitated by the elimination of expensive laser systems and the use of more affordable materials from metal injection molding (MIM), along with seamless integration into similar manufacturing process chains. Unlike L/E-PBF, MBJ does not use lasers or electron beams to fuse metal particles; instead, it employs a liquid binder to bond them at room temperature. The parts, known as green parts, undergo debinding and sintering where the binder is removed, and the metal particles are fused through diffusion processes to form nearly dense components [1,2]. MBJ has gained significant traction as an innovative additive manufacturing process, offering substantial benefits over traditional manufacturing methods. The promise of MBJ especially for medical technology is underscored by its ability to produce parts potentially with lower costs and enhanced geometric accuracy compared to traditional L/E-PBF processes [3,4]. MBJ facilitates the production of intricate parts without the need for support structures, avoids thermal stresses, prevents shape distortion and cracking, and does not induce undesirable microstructural changes or material loss, thus ensuring high material recycling efficiency and cost-effectiveness, especially for expensive materials such as titanium [5,6]. Despite these promising advancements and the potential for significant cost reductions in medical technology, MBJ has not yet fully realized its potential in the market. The initial costs for MBJ systems remain comparable to those of L/E-PBF, and the industry still lacks medically certified process routes for biomaterials such as titanium, as well as suitable powder conditioning strategies that would allow for the direct use of MIM powders in binder jetting processes.

In a previous study the authors already addressed these potentials by developing advanced powder conditioning strategies, aimed at optimizing moisture content and respective powder flowability to use (MIM-like) low powder size distributions for better sintering kinetics, better integrability into MIM process routes and enhance the overall quality of MBJ green parts [7]. In order to understand how these new conditioning strategies (with drying temperatures of up to 200°C), as well as additional process steps such as sieving or curing affect possible impurities as well as powder size distributions, flowability and the surface quality of the subsequent green parts, these relationships are examined in more detail in this publication. This contribution is therefore part of a holistic examination of the entire MBJ process chain for Ti-6Al-4V, from powder to green part, focusing specifically on potentials, challenges and strategies associated with green part manufacturing, powder conditioning, powder recycling and green part curing. By integrating advanced conditioning strategies developed in our previous work, this research contributes to refining process parameters that maintain material properties while minimizing environmental impacts thru improved material efficiency, thereby supporting the broader adoption and technical viability of MBJ for medical technology.

Titanium and its alloys remain the materials of choice for biomedical applications and prostheses due to their biocompatibility, non-toxicity, and superior mechanical properties [8,9]. Due to their relevance in medical technology, titanium and titanium alloys like Ti-6Al-4V are extensively studied for their application in Metal Binder Jetting (MBJ) and are the focus of numerous research publications. Simchi et al. addressed challenges in achieving high-density and fine microstructural control, emphasizing the importance of optimizing powder particle size and printing conditions. The study demonstrates that achieving parts with mechanical properties comparable to those produced by MIM is possible through tailored sintering strategies. Overall, it provides valuable insights into improving the quality and functionality of 3D printed titanium parts for biomedical applications [10]. Stevens et al. investigated the impact of post-processing on the density of titanium alloy parts

*corresponding author, kevin.janzen@iapt.fraunhofer.de

using MBJ. The study highlights how density varies within parts, often lower at edges and higher at areas of significant curvature, attributed to variabilities in the printing process such as binder and powder distribution. It discusses how these factors influence the coordination number and densification rates during sintering, which ultimately affects the mechanical properties and structural integrity of the final parts. The research emphasizes the need for understanding and controlling these parameters to improve the quality and consistency of binder jetted metal parts [11]. Tischel et al. developed a phenomenological densification model for predicting sintering behavior in Ti-6Al-4V MBJ samples. The study details the calibration of this model using experimental data from dilatometry experiments, highlighting the importance of understanding anisotropic shrinkage and thermal expansion to enhance manufacturing precision. Key findings demonstrate good alignment between model predictions and experimental sintering outcomes, emphasizing the model's utility in optimizing sintering processes for achieving desired density and mechanical properties [12]. Literature indicates that oxygen and nitrogen incorporation during thermal post-processing and during handling under ambient atmosphere can significantly alter the microstructure of Ti-6Al-4V, potentially degrading its mechanical properties (especially elongation) [13,14].

Thus, this study aims to evaluate the effectiveness of the previously developed conditioning strategies by investigating oxygen and nitrogen uptake at elevated temperatures, a critical factor for maintaining the alloy's properties across multiple recycling cycles. Powder recycling in MBJ in general is a subject of growing interest, as maintaining the quality of recycled powder is imperative for the economic and environmental sustainability of the process. To date, there is no literature that deals specifically with the powder recycling of titanium alloys for MBJ. However, there is some work on other materials (especially stainless steels). Mirzababaei et al. examined the recyclability of 316L stainless steel powder. The study highlights that after recycling the powder up to 16 times, there was an increase in coarse particles and a decrease in small particles, with minimal oxygen content change, suggesting a negligible effect on the chemical properties. Despite these changes in particle size distribution, the mechanical properties of the parts made from recycled powder were similar to those made from fresh powder [15]. Zissel et al. investigated the reusability of 17-4 PH stainless steel powder in MBJ. Their study examined how repeated reuse affects the powder's physical and chemical properties, its influence on print quality and the impact of inert and reducing atmospheres during curing. It found that despite multiple reuse cycles, the mechanical properties of parts produced remain consistent, although there are slight changes in particle size distribution and increased oxygen content [16]. Seyda et al. examined the changes in Ti-6Al-4V powder properties due to repeated use in L-PBF. It was shown that with multiple recycling cycles, Ti-6Al-4V powder undergoes coarsening of particles and increased flowability, which significantly affects the quality of the laser-melted parts. The study links these aging characteristics directly to alterations in the density, porosity, and mechanical properties of the produced components, showing a decrease in porosity and variations in density as the powder ages [17]. Lutter-Günther et al. also enhanced resource efficiency in L-PBF through advanced powder recycling strategies. Their study introduces two interrelated models: a powder reuse cycle calculation model, and a resource and energy consumption model refined for L-PBF processes. These models assess the global warming potential (GWP) of L-PBF parts, considering different recycling strategies and material losses. The findings indicate that the optimal reuse of powder can substantially lower the GWP-impact of the L-PBF process, which emphasizes the environmental benefits of effective powder recycling strategies [18].

The aim of this study is to quantify the effects of recycling titanium powder in the MBJ process, specifically focusing on both the powder and the green part properties. The goal is to contribute to optimizing the MBJ process chain and to establish guidelines for recycling titanium powder that could potentially be adopted for medical applications. This follows a detailed exploration of powder conditioning in [7] and highlights the significance of recycling non-bound powder to make MBJ more cost-effective and environmentally friendly, thus facilitating the industrialization of the process.

Materials & Methods

The design of the experiments followed two separate strategies:

1. Influences due to recycling over the entire process chain: A total of four cycles were considered here, whereby all process steps (powder conditioning, sieving, binder jetting, curing, depowdering) were run through each time (see Fig. 1, left).
2. Thermal influences due to recycling: Here the investigations were limited to the purely thermal influences, i.e. powder conditioning and curing. A total of 15 cycles were considered here (see Fig. 1, right).

These two strategies make it possible to quantify the thermal influences in particular for a higher count of cycles, as this would not be economically feasible due to the quantities of powder required for the entire process chain due to losses during the process.

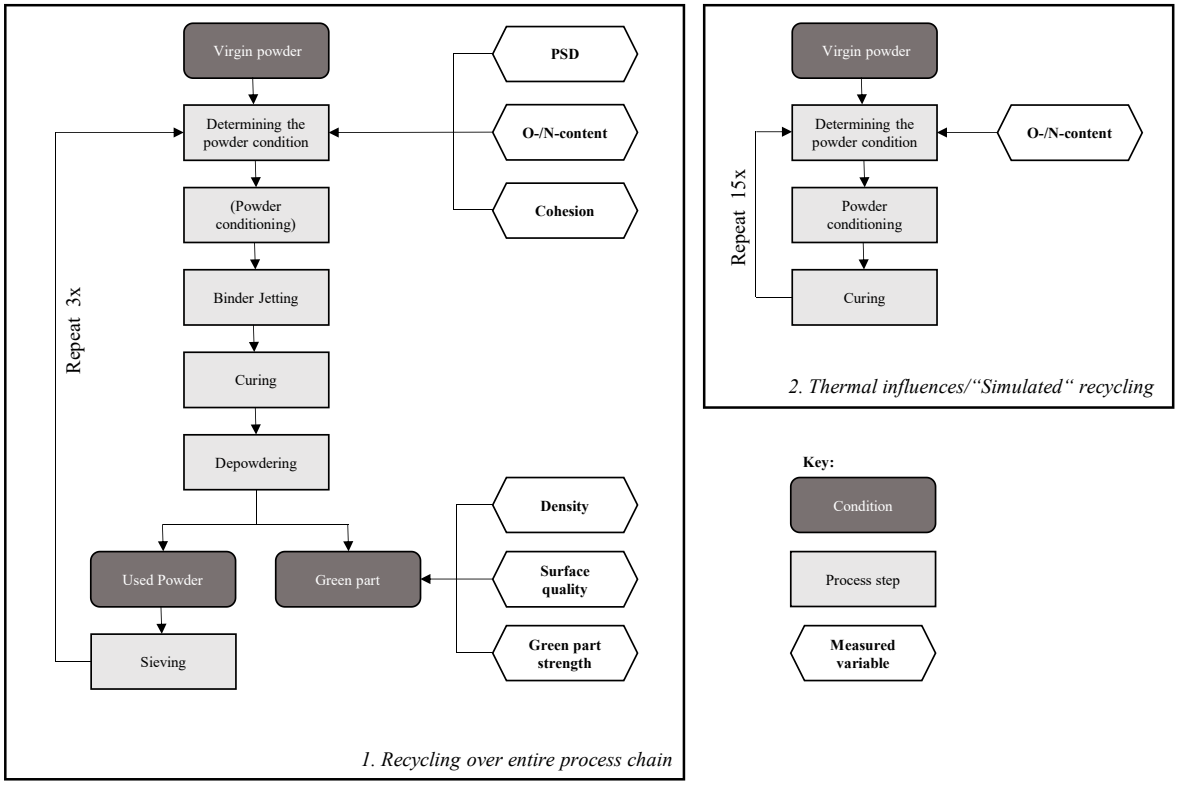

Fig. 1 Study design

Materials

The study used 10 kg of virgin plasma-atomized spherical Ti-6Al-4V powder supplied by Tekna Advanced Materials, Inc. (Sherbrooke, Canada) with increased oxygen content (TEKMAT™Ti64 25/5 HO). The most important characteristic properties of the powder are shown in Table 1. Only powder from a single batch was used for the experiments.

Table 1 Properties of the investigated powder

Alloy	Supplier	D_{10} (µm)	D_{50} (µm)	D_{90} (µm)	Apparent Density (g/cm³)	Tap Density (g/cm³)	Oxygen content [%]	Water content as received (ppm)
Ti-6Al-4V	Tekna	9.43 [1]	15.6 [1]	21.3 [1]	≥2.1 [2]	≥2.7 [2]	0.2-0.3[2]	49,5[3]

[1] Measured using dynamic image analysis; [2] manufacturer information; apparent density according to ASTM B527 and Tap density according to ASTM B417; [3] measured using Karl-Fischer-titration.

Powder Characterization

Powder condition characterization involved measurements of particle size distribution (PSD) and sphericity using a Camsizer X2 (Microtrac Retsch Gmbh, Haan, Germany) for dynamic image analysis following DIN ISO 13322-2. The water content of the virgin powder was also determined by Karl-Fischer-Titration (KFT) utilizing a Metrohm 899 Coulometer (Metrohm GmbH & Co. KG, Filderstadt, Germany) before the powder was dried using the conditioning strategies from [7]. The water content was measured as an example at various points in the process cycle, but was deliberately not included as a target value, as it depends on the duration of the individual process steps, which cannot always be kept constant. Given the inherent tendency of titanium alloys to absorb oxygen and nitrogen, and considering the exposure of the powder to temperatures up to 200 °C during conditioning and curing, the levels of these elements were quantified using infrared absorption for oxygen and thermal conductivity cells for nitrogen. To assess flowability, the dynamic angle of repose and the cohesion index were measured using rotating drum analysis (GranuDrum by GranuTools, Awans, Belgium), with adjustments made for the rotational speed of the drum to align with the MBJ printer's coating speed, producing a comprehensive set of data from multiple images and rotational directions to ensure accuracy despite the inherent challenges of the powder's flow characteristics. For this, 80 images were taken for each measurement. The direction of rotation of the drum is changed after 40 images. Also, three powder samples are measured, so a total of 240 measured values can be averaged for the dynamic angle of repose (α). For the cohesion index (CI), only two measured values are collected per measurement, one for each

direction of rotation. The result is therefore averaged from six measured values. According to the manufacturer, the measurement accuracy of the method is 1.67 %.

Green Part Characterization

To characterize green parts the following target values were used: green part density, dimensional accuracy, surface quality and green part strength. The density is often determined using the Archimedes method or via the porosity of micrographs. However, both measuring methods cannot be used for green parts due to the water-soluble binder. Instead, optical measurement using fringe projection was used (VR-6200 by Keyence Corporation, Osaka, Japan). Fringe projection is a triangulation method in which the component is illuminated with structured light, i.e. the fringes. A camera records the diffraction of the stripes. The position of the camera and the projector in relation to each other is known so that the component surface can be triangulated. This allows the volume of the body to be determined. The measuring accuracy of the profilometer that was used is 4 µm for twenty-fold magnification and measurement using the macro camera. In addition to the calibration of the measuring device, only the room lighting and the reference surface from which the measurement is taken have an influence on the accuracy of the measurement. The lighting is therefore kept constant and the object table is used as the measuring surface. The weight of the sample was measured by weighing using a precision balance (PRACTUM 124-1S by Sartorius, Göttingen, Germany) so that it is possible to determine an accurate value for the geometric green density. The dimensional accuracy and surface roughness were also determined optically via fringe projection. Finally, a bending test was carried out in accordance with DIN EN ISO 3995 to determine the green part strength. The standard, which was actually created for metallic pressed parts, is consulted for green parts due to the lack of other standards. The green part was placed on two support cylinders at a distance of 25 mm and loaded centrally for bending. A tensile/compression testing machine (ZwickRoell 10kN by Zwick Roell, Ulm, Germany) with an appropriate setup was used for this.

Powder conditioning

The powder conditioning strategy developed in [7] must be adapted for the correspondingly larger quantity of powder. The powder was divided into two large stainless-steel tubs. As the heat transfer to the powder is presumably decisive for drying, the quantity of powder to be dried in g/cm^2 of the heat transfer surface was used as the reference value for the test series. This corresponds to 2.1 g/cm² for the powder conditioning study [7] and 5.8 g/cm^2 for the present recycling study, i.e. an increase by a factor of 2.76. According to the model created in 7), a drying time of 6 h at 200 °C is required for a water content of 21.8 ppm. For the larger quantity, this would be 16.6 h at 200 $°C$. The powder was therefore dried overnight and the water content is then determined again. This resulted in a water content of 21.5 ppm with a range of 2.0 ppm as a starting value. After the first cycle following the entire process chain (Fig. 1, left) another KFT measurement was done and determined a water content of 21.8 ppm. As this difference is only very insignificant, it was assumed that the curing process and the heated powder magazine of the MBJ system hinder a significant increase in water content, provided that the powder is not subjected to intermediate storage. Powder conditioning was therefore only carried out for the first cycle.

Binder Jetting

MBJ was carried out on a Digital Metal (now Markforged, Inc., Watertown, NY, USA) DM P2500 system. The printing parameters are listed in Table 2:

Table 2 Metal binder jetting parameters

Parameter	Value
Binder	Digital Metal C20 Ink
Layer thickness	42 µm
Print box temperature	80 °C
Powder magazine temperature	70 °C
Print speed	200 mm/s
Powder application speed	30 mm/s

The specimens for MBJ were selected based on the sizes to be measured. A simple rectangular bending specimen is required for the bending test. The edge dimensions for the specimen are 30x12x9 mm. A cube with an edge length of 10 mm was selected for measuring surface quality and dimensional accuracy. For determining the volume by means of fringe light projection, a body that can be illuminated well from all sides was needed. A pyramid with a square base and an edge length of 14 mm was selected for this purpose (see Fig. 2). Small sinter samples were also produced for further investigations. Four samples were printed per layer in order to be able to average at least three samples per measurement. The samples were evenly distributed in the print bed.

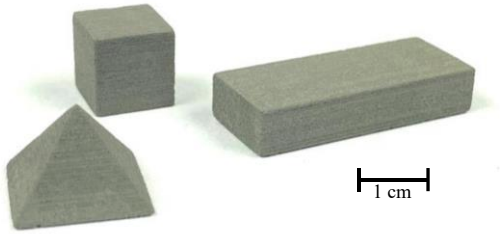

Fig. 2 Printed green parts

Curing

After printing the samples were cured in a TR-242RN furnace (Nabertherm, GmbH, Lilienthal, Germany). The cycle used for this is shown in Fig. 3. It is divided into a ramp time (R), a holding time (H) and the cooling time (A).

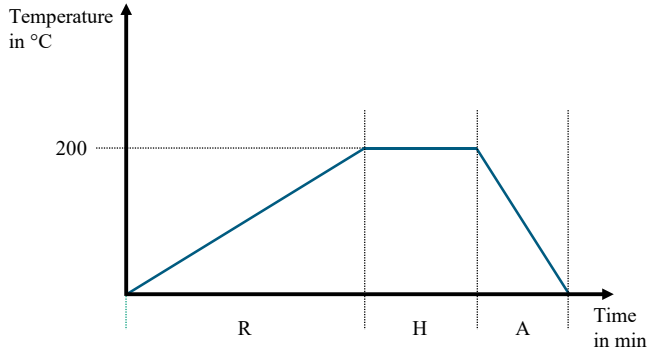

Fig. 3 Curing cycle principle

The ramp time was determined as specified by the binder manufacturer (Markforged) and depends on the number of layers (L) and the quantity of binder used (I):

$$R = I + 0.3 \times L$$

The holding time was also determined by the number of layers. The following applies: L<300 → H= 1 h; 300<L<600 → H= 2 h; L>600 → H= 3 h. The cooling time was always two hours and the temperature was set to 200 °C for each cycle.

Depowdering

After curing, the green parts were depowdered. This step was carried out under nitrogen atmosphere in a glovebox. The components were only depowdered with a brush. Care was taken to ensure that the different component layers were separated so that the components in the lowest layer could always be compared with each other for each recycling pass.

Sieving

After depowdering, the loose powder was then collected, filled back into steel powder bottles and sieved under argon gas in a custom-made sieving station. The sieving station is completely powder-tight for safety reasons and was flooded with argon gas before use. After opening the corresponding valves, the powder from the used powder bottle is fed directly onto the sieve. A linear conveyor moves the powder along a screen and collects it in a fine grain outlet. Powder agglomerations are filtered out via a coarse grain outlet.

Results & Discussion

In this section, the results of the recycling study are presented and discussed one after the other. The dried new powder and the recycled powders and their green parts are always discussed. Where appropriate, comparisons are also made with the "simulated" recycled powder (see Fig. 1, right). In the following, the different powders are labeled according to the scheme "1rp" (once recycled powder) and so on. The recycling processes that only cover the thermal process steps curing and conditioning are labeled "simulated-recycled powder". The repeatability is determined by averaging the samples several times. Reproducibility is discussed if the measuring device has an operator-dependent measuring principle, but is not determined. Measurement accuracy is presented for each method and included in the results. Measures to increase precision are presented in order to produce the most accurate measurement results possible.

Particle size distribution and sphericity

Table 3 shows the results of the PSD and their ranges. The measurement accuracy of the method with current calibration is 0.1 µm. Considering the range, no significant increase in the D_{10} value and thus loss of the fine fraction can be determined. On the other hand, a slight increase in the D_{50} and D_{90} values can be seen.

Table 3 Particle sizes and sphericity for different numbers of recycling cycles

Cycles	D_{10} (µm)	D_{50} (µm)	D_{90} (µm)	Sphericity
Virgin	9.43	15.60	21.30	0.880
1rp	9.57	15.77	21.33	0.880
2rp	9.40	15.63	21.50	0.880
3rp	9.53	15.90	22.07	0.880
4rp	9.40	15.80	21.70	0.881

O-/N-content

Fig. 4 shows the measured oxygen content for the respective recycling stage. There is no significant change in the oxygen content between the individual recycling steps, but all recycled powders have a higher content than the conditioned virgin powder. The increase is between 0.047 and 0.06 wt.%. This indicates a purely passive oxidation and is in line with the literature, which suggests that active oxidation only occurs from around 300°C [19].

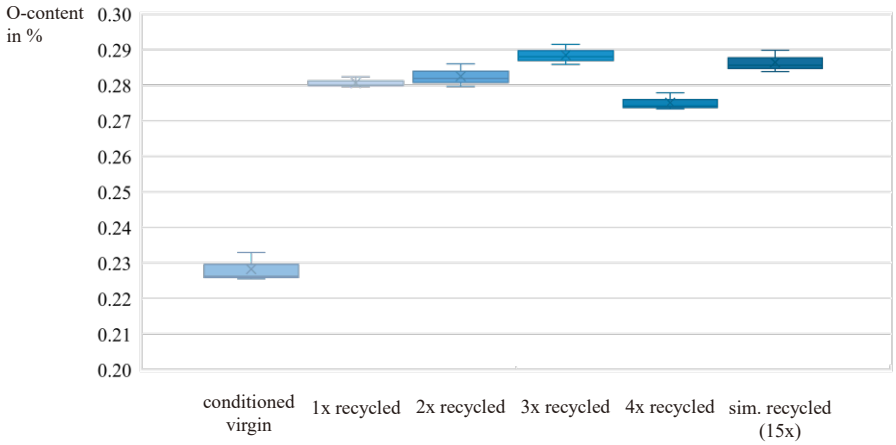

Fig. 4 Oxygen content for the respective recycling stages

A similar behavior can be observed for the nitrogen content (Fig. 5). The increase is between 0.006 and 0.008 wt.%.

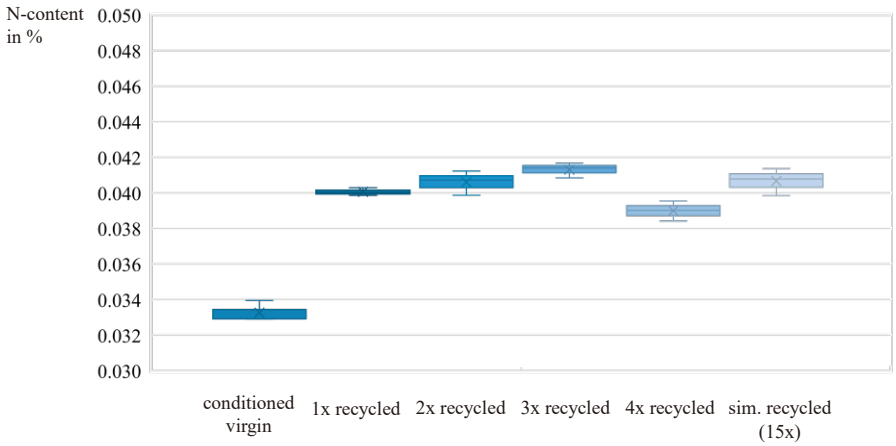

Fig. 5 Nitrogen content for the respective recycling stages

In the presence of oxygen and nitrogen, the oxide layer is preferentially formed. The layer certainly hinders the diffusion of N, but perhaps does not suppress it completely. However, since a significant increase can only be seen after the first recycling, some protective layer seems to form (e.g. an ON mixed layer). Following the principle of the oxygen equivalent, nitrogen is twice as effective for embrittlement as oxygen [14]. Yet the pick-ups measured for both oxygen and nitrogen are anything but critical for the application and do not hinder powder recycling.

Cohesion

The measured values for the cohesion index and the dynamic angle of repose are shown in Table 4.

Table 4 Dynamic angle of repose and cohesion index in different recycling stages

Cycles	α (°)	Range of α (°)	CI	Range of CI
Virgin	33.84	2.30	14.0	1.6
1rp	30.10	2.50	11.5	1.2
2rp	31.00	2.10	11.8	0.6
3rp	32.00	2.60	12.8	0.6
4rp	31.10	2.00	10.9	0.5

The extensive range makes it difficult to observe a definitive shift in the dynamic angle of repose α during the recycling steps. Nonetheless, a noticeable decrease of 3.1 in the cohesion index is evident, which suggests a slight improvement in flow properties.

Green part density

From the density values (ρ), no significant change in density can initially be seen over the recycling stages (see Fig. 6). However, upon examining the measurement ranges, it becomes evident that they increase with the number of recycling processes. This indicates a certain influence of powder recycling on process stability.

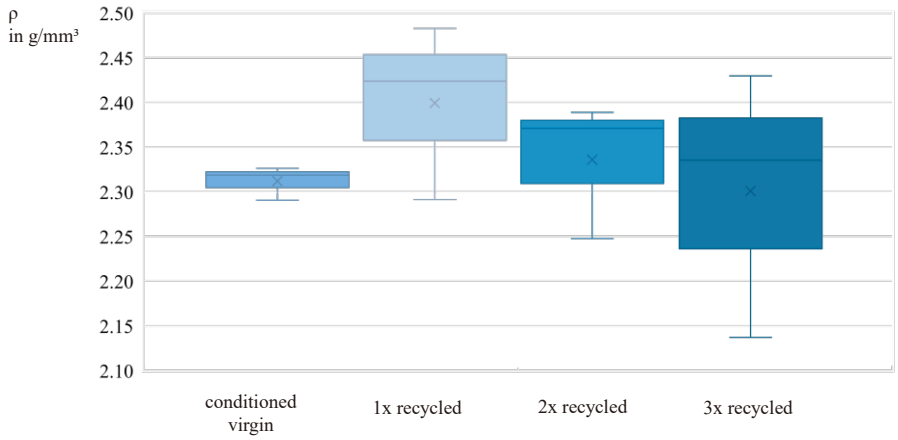

Fig. 6 Green part density for the respective recycling stages

Surface quality

The surface roughness is measured with the micro-camera and a forty-fold magnification, resulting in a measurement accuracy of 2 µm. Both S_a and S_z are determined. However, the mean roughness depth S_a is more suitable for the evaluation, as the absolute roughness depth S_z has very large ranges of several hundred µm. As the green parts are very sensitive, they may have been damaged during powder removal or handling, which is why small scratches have a strong influence on the surface quality result. With the mean roughness depth, these are less significant and the ranges are significantly lower. Here too, no significant difference in surface quality can be seen between the recycling cycles and also in this case the range of measured values increases for the recycled powder (see Fig. 7).

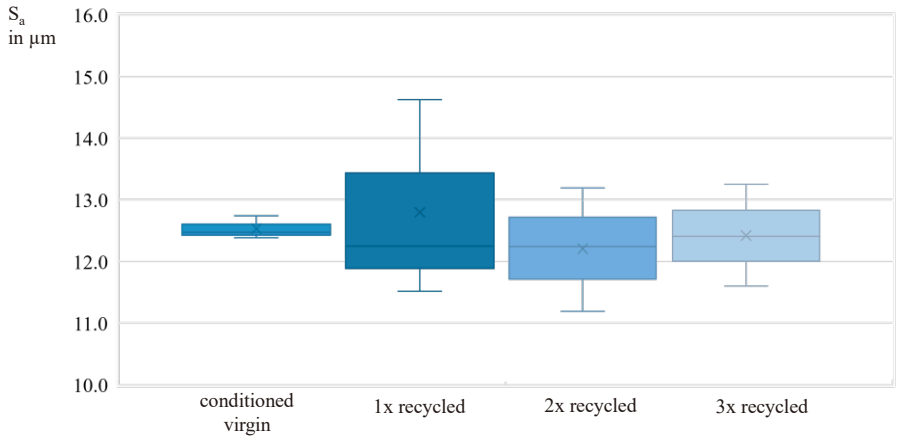

Fig. 7 Mean roughness depth S_a for the respective recycling stages

Conclusion

This extensive investigation into the recycling of Ti-6Al-4V powder within the framework of MBJ underscores its considerable potential to boost both economic efficiency and environmental sustainability in additive manufacturing, particularly within the medical sector. The study revealed that even after recycling the Ti-6Al-4V powder four times, changes in particle size distribution were minimal, flow properties were enhanced, and importantly, there was no substantial pickup of oxygen or nitrogen even after 15 times of conditioning and curing. This latter finding supports our previous powder conditioning study [7], reinforcing the effectiveness of advanced conditioning strategies that maintain the quality and performance of MBJ processes. The research supports the broader adoption of titanium powder recycling practices, which promise to revolutionize production methods in industries requiring high precision and integrity in material properties. Moreover, it sets a foundation for further research aimed at refining recycling protocols and broadening the range of materials that can be sustainably reused, thereby fostering wider industrial acceptance of sustainable practices in metal additive manufacturing.

Looking forward, it is imperative to conduct a detailed examination of the curing process, as it is the last critical step to represent a holistic approach for the use of titanium alloys in MBJ. A systematic exploration of how curing conditions interact with powder and green part qualities will enable the development of more detailed and effective guidelines for the complete MBJ process chain with titanium alloys. Such targeted research will not only deepen our comprehension of the involved thermal dynamics but will also facilitate the creation of an integrated framework to substantially enhance the efficiency and sustainability of MBJ with titanium alloys. This approach is especially crucial in medical applications where stringent quality standards must be met. By ensuring the process chain is optimized for both environmental and cost considerations, and meets the high-quality standards required in medical manufacturing, this future work will further solidify the role of advanced manufacturing solutions in industry.

References

1) S. Mirzababaei, S. Pasebani: Journal of Manufacturing and Materials Processing, **3** (2019), 82.

2) M. Ziaee, N. Crane: Additive Manufacturing, **28** (2019), 781-801.

3) K. Janzen, P. Groß, P. Imgrund, C. Emmelmann: World PM2022 Proceedings, (2022).

4) K. Janzen, K. Kallies: Transactions on Additive Manufacturing Meets Medicine, (2023).

5) I. Gibson, D. Rosen, B. Stucker, M. Khorasani: Additive Manufacturing Technologies, (2021), 685.

6) M. Munsch, M. Schmidt-Lehr, E. Wycisk, T. Führer: Metal Additive Manufacturing with sinter-based technologies, (2018).

7) K. Janzen, K. Kallies, L. Waalkes, P. Imgrund, C. Emmelmann: Materials (Basel, Switzerland), **17** (2024).

8) M. Niinomi: Metallurgical and Materials Transactions A, **33** (2002), 477-486.

9) H. Rack, J. Qazi: Materials Science and Engineering: C, **26** (2006), 1269-1277.

10) A. Simchi, F. Petzoldt, T. Hartwig, S. Hein, B. Barthel, L. Reineke: The International Journal of Advanced Manufacturing Technology, **127** (2023), 1541-1558.

11) E. Stevens, S. Schloder, E. Bono, D. Schmidt, M. Chmielus: Additive Manufacturing, **22** (2018), 746-752.

12) F. Tischel, L. Reineke, J. Alrashdan, V. Ploshikhin, (2023).

13) T. Ebel, V. Friederici, P. Imgrund, T. Hartwig, **67**, 337-360.

14) U. Zwicker: Titan und Titanlegierungen, (1974).

15) S. Mirzababaei, B. Paul, S. Pasebani: JOM, **72** (2020), 3070-3079.

16) K. Zissel, E. Quejido, T. Deckers, P. Forêt, E. Hryha: World PM2022 Proceedings,

17) V. Seyda, N. Kaufmann, C. Emmelmann: 1875-3892, **39** (2012), 425-431.

18) M. Lutter-Günther, C. Gebbe, T. Kamps, C. Seidel, G. Reinhart: Production Engineering, **12** (2018), 377-389.

19) G. Lütjering, J. Williams: Titanium, 2, (2007), 442.

Received June 20, 2024; Revised August 22, 2024; Accepted September 9, 2024